and the tube then placed into a constant temperature quartz vessel, located inside of the Rayonet reactor. In all cases, the irradiation time used was 2 h.

Isolation and Characterization of Poly(methacrylic acid). Typically, an aqueous dispersion of polymerized DODAM containing 306.7 mg (0.48 mmol) of surfactant (a combination of two separate preparations that had been polymerized via UV irradiation at 30 °C) was freeze-dried and the residue dispersed in 50 mL of absolute ethanol. After addition of 1 mL of concentrated HCl, the dispersion yielded a clear solution. The solution was then concentrated under reduced pressure, redissolved in 50 mL of ethanol, and reduced to dryness. This procedure was repeated 2 times and the residue then dried under high vacuum [25 °C, 12 h (0.05 mmHg)]. A minimum volume of ethanol (ca. 2 mL) was added to dissolve the residue, and *n*-hexane was then added in a dropwise fashion. During the addition of hexane, the mixture was gently shaken by hand, in order to precipitate poly(methacrylic acid). The crude yield of polymer was 39.8 mg (96%). Further purification of the polymer was carried out by repeating this precipitation procedure 3 times. The final product [33.2 mg (80%)] exhibited an IR spectrum which was identical with that of an authentic sample of poly(methacrylic acid). Using similar procedures, an aqueous dispersion containing 310 mg (0.49 mmol) of DODAM, which had been photopolymerized at 60 °C, afforded crude and purified yields of poly(methacrylic acid) of 33.4 mg (80%) and 23.5 mg (56%), respectively.

Attempted Polymerization of DODAM Using Radical Initiators in the Vesicle State, in Solution, and in the Bulk Phase. Addition of 5 mol % AIBN or ACVA to aqueous dispersions of DODAM (1 mg/mL), followed by brief sonication (2 min), heating (7 days, 60 °C), and freeze-drying afforded only starting monomer as indicated by its ^{1}H NMR spectrum in $CDCl_3$. Similarly, attempted polymerization of 644 mg of DODAM dissolved in 0.5 mL of absolute ethanol containing 8.2 mg (5 mol %) of AIBN, for 3 days at 60 °C, or of DODAM in the neat state (bulk polymerization), for 3 days at 75 °C, afforded only unreacted starting monomer.

Captured Volume and Permeability. Typically, a vesicle dispersion was prepared from 15 mg of DODAM in 2.25 mL of distilled water containing 15 μCi of sucrose by using procedures similar to those described above. After sonication, the dispersion was divided into three equal portions; one was photopolymerized at 30 °C and one at 60 °C. An aliquot of each portion (50 μL) was withdrawn and analyzed for nitrogen and sucrose content. Additional aliquots (0.5 mL) were then filtered through a 10 mm diameter column which was packed with water-swollen Sephadex G-50 (made from 2.0 g of dry Sephadex). Collected fractions (1.16 mL) were analyzed for radioactivity and nitrogen content. In all cases, a well-defined separation between free and vesicle-entrapped sucrose (void volume) was obtained. The ratio of entrapped sucrose/free sucrose (R) represents the counts per minute (cpm) in the void volume of the column divided by the total cpm added to the column. The apparent internal or captured volume (V) has been calculated by dividing R by the concentration of surfactant, [DODAM], in the vesicle state. The value of [DODAM] equals the moles of nitrogen/liter of the dispersion applied to the filtration column multiplied by the percentage of nitrogen recovered in the void volume. The extent of sucrose *adsorption* to preformed nonpolymerized and polymerized DODAM vesicles was determined by adding [^{14}C]sucrose to the appropriate vesicle dispersion, incubating the mixture for 0.5 h at room temperature, and then filtering the dispersion through a Sephadex G-50 column. The amount of adsorbed sucrose in the void volume was then expressed as an "adsorbed" captured volume (V_a). Specific V_a values obtained for nonpolymerized, 30°-polymerized, and 60°-polymerized vesicles are 0.22, 0.06, and 0.09 L/mol, respectively. The true captured volumes of these vesicles (V_{in}), defined as $V_{in} = V - V_a$, are reported in Table II. Dialysis experiments were carried out either at 30 or 60 °C, using procedures similar to those previously described.[13] Typically, 2.0 mL of a gel-filtered vesicle dispersion (immediately after filtration) was dialyzed against 200 mL of distilled water at the specified temperature.

Film-Balance Experiments. Force–area isotherms were recorded by using a computerized MGW Lauda film balance at 22 °C. Water that was used as a subphase was deionized and freshly distilled in an all-glass apparatus. Surfactants were spread onto the water surfaces (600 cm^2) from 9:1 hexane/ethanol solutions (ca. 0.2 mg/mL) by using a 10- or 50-μL glass syringe. Monolayers were compressed at a rate of 20 cm^2/min. Photopolymerization reactions were carried out by irradiating the monolayers with a single UV Rayonet lamp (254 nm) from a distance of 7 cm under an argon atmosphere.

Acknowledgment. We are grateful to Drs. Jae-Sup Shin and Jitender Khurana for valuable technical assistance.

Registry No. DODAM, 7524-96-1; PDODAM, 89346-16-7; sucrose, 57-50-1.

Stoichiometry and Structural Effects in Alcohol Chemisorption/Temperature-Programmed Desorption on MoO_3[†]

W. E. Farneth,* R. H. Staley, and A. W. Sleight

Contribution from E. I. du Pont de Nemours & Company, Central Research and Development Department, Experimental Station 356/B37, Wilmington, Delaware 19898.
Received August 22, 1985

Abstract: The mechanism of alcohol oxidation over MoO_3 has been examined by using temperature-programmed desorption spectroscopy (TPD) with simultaneous microbalance and mass spectral detection. Two types of experiments are reported. The alcohol structure has been varied over the sequence methyl, ethyl, 2-propyl, *tert*-butyl, and systematic changes in the amount of chemisorption, the peak desorption temperature, and the nature of the products have been observed. The amount of water produced during chemisorption of ethyl alcohol on MoO_3 at room temperature has been measured. This determination makes it possible to estimate the coverage of alkoxy groups after the chemisorption stage. The fate of these ethoxy groups during subsequent TPD can be followed. A stoichiometric accounting of both acetaldehyde production and catalyst reduction can be made.

In a previous publication, we have described the use of temperature-programmed desorption spectroscopy (TPD) with simultaneous microbalance and mass spectral detection as a means of studying heterogeneous redox chemistry.[1] It was demonstrated that each of the essential elements of the overall process, adsorption of the substrate on the solid catalyst, chemical reaction of the adsorbate, and reoxidation of the catalyst, could be productively studied by using this instrumentation. In the particular case of methanol partial oxidation to formaldehyde over MoO_3, surface

[†] In this paper the periodic group notation in parentheses is in accord with recent actions by IUPAC and ACS nomenclature committees. A and B notation is eliminated because of wide confusion. Groups IA and IIA become groups 1 and 2. The d-transition elements comprise groups 3 through 12, and the p-block elements comprise groups 13 through 18. (Note that the former Roman number designation is preserved in the last digit of the numbering: e.g., III → 3 and 13.)

(1) Farneth, W. E.; Ohuchi, F.; Staley, R. H.; Chowdhry, U.; Sleight, A. W. *J. Phys. Chem.* **1985**, *89*, 2493.

0002-7863/86/1508-2327$01.50/0

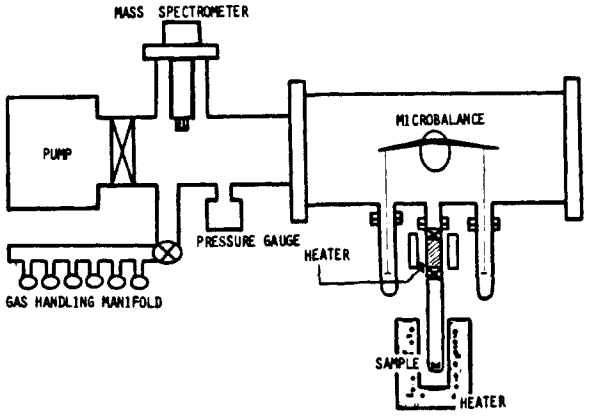

Figure 1. Schematic of microbalance/TPD apparatus showing two-tiered sample holder for H_2O production experiments.

intermediate concentrations and Arrhenius parameters obtained by TPD could be used to quantitatively model reactor data. This close link to reactor studies implies that conclusions about the mechanism under the relatively well-defined and well-controlled conditions of high-vacuum temperature-programmed reaction spectroscopy can be directly applied to understanding the process chemistry.

In this paper, we further examine the heterogeneous redox chemistry of MoO_3. Two types of experiments are reported. The first is a comprehensive look at the sensitivity of the TPD behavior to alcohol structure. Variation of the alcohol structure over the sequence methyl, ethyl, 2-propyl, *tert*-butyl results in systematic changes in the amount of chemisorption, the peak desorption temperature, and the nature of the products. The second is a determination of the amount of H_2O produced during chemisorption of ethanol on MoO_3 at room temperature. These data in combination with the microgravimetric and mass spectroscopy measurements of the TPD experiment are used to quantitatively map out the stoichiometry of the adsorption and chemical reaction steps in the overall redox mechanism.

Experimental Section

The instrumentation has been described previously.[1] Experiments were carried out as follows: The catalyst as a pressed pellet of ~200-mg mass was placed in the sample pan of a Cahn UHV R.G. microbalance mounted within a high-vacuum enclosure. Typical pretreatment involved heating to 400 °C at 1×10^{-8} torr followed by oxidation at the same temperature in 10 torr of oxygen. Chemisorption occurs during exposure of the pretreated sample to alcohol vapor at varying pressures, times, and temperatures. The amount of chemisorption was measured gravimetrically as the stable weight gain after pump out. Weight changes are also followed during TPD and reoxidation. For temperature-programmed reaction/desorption, the catalyst chamber can be enclosed in a furnace and heated to 400 °C. Effluent gases are monitored with a UTI 100 quadrupole mass spectrometer.

As a variation of this procedure, in certain cases, a two-tiered sample holder was mounted to the vacuum chamber that encloses the microbalance. The two tiers could be heated independently and were separated from one another, and as a unit from the vacuum chamber, by high-vacuum shut-off valves. The bottom chamber was a cylinder of heavy-walled Pyrex tubing capped through a glass-to-metal seal with a minicon flange. The upper chamber was a $^1/_4$-in. o.d. stainless steel tube packed with Linde 3-Å molecular sieves (50 mg) and glass wool. The MoO_3 catalyst pellet could be loaded into the bottom chamber. Effluent gases from the botton tier must pass through the top tier during pump out (Figure 1). The basis of the experiment is the well-known utility of 3-Å sieves as an ethyl alcohol drying agent.[2] Both the MoO_3 catalyst and the sieves were pretreated by heating in vacuum to 400 °C. The MoO_3 was also oxidized by exposure to O_2 at this temperature.

In an experiment to measure H_2O production during chemisorption, dried, degassed ethyl alcohol vapor was expanded into the two-tiered sample holder from the manifold, and the sample holder was isolated from the main vacuum chamber. Exposures varying from 0.01 torr/12 min to 10 torr/2 h were examined. Following exposure, the system was slowly pumped down to the background pressure, the valve to the bottom chamber closed, and the top chamber heated rapidly (15 min to 400 °C) to desorb any material adsorbed on the sieves. The desorption process was followed by mass spectroscopy. The amount of H_2O desorbed was determined by integration of the m/e 18 profile.

(2) Feiser, L. F.; Feiser, M., *Reagents for Organic Synthesis*; Wiley: New York, 1967; Vol. 1, p 703.

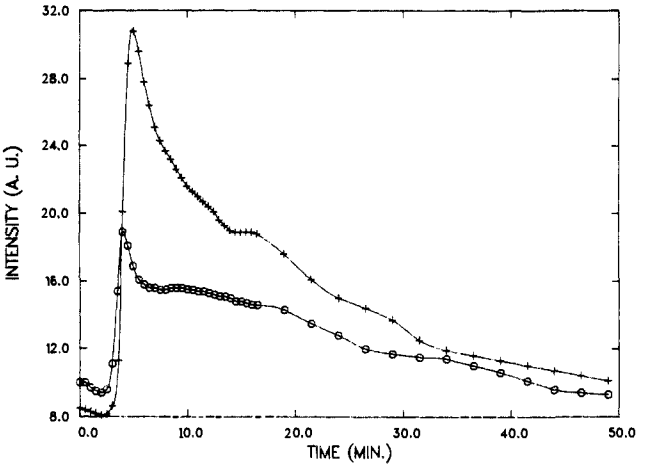

Figure 2. Intensity of m/e 18 vs. time in desorption for experimental and control conditions: (+) with MoO_3 in bottom chamber, (O) without MoO_3 in bottom chamber.

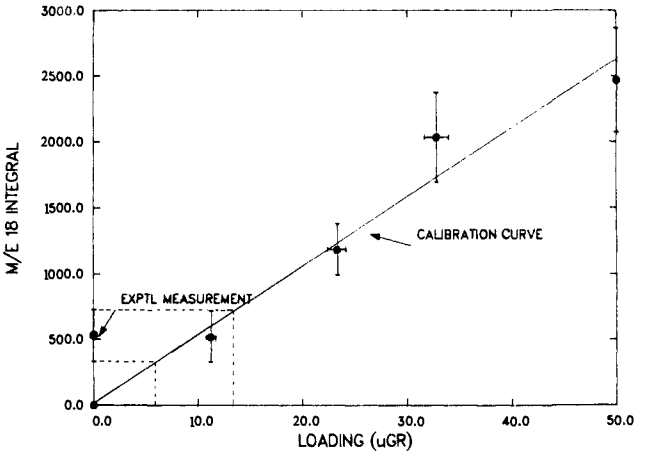

Figure 3. Calibration curve for mass spectral integral of m/e 18 peak vs. desorbed mass. Experimental point is the mean of three experiments at an ethyl alcohol exposure of 120 torr-min.

A number of control experiments have been performed. Four in particular are not worthy: 1. When the experiment is carried out without MoO_3 in the bottom chamber, H_2O is still observed. However, the amount of water is significantly reduced from the experimental condition. Data from experiments with and without MoO_3 are shown in Figure 2. Controls of this kind were run for each ethyl alcohol exposure. All reported data represent the difference between the m/e 18 integrals with and without MoO_3 at a given exposure. 2. m/e values associated with water (m/e 18, 17) are the only masses that show significant differences between the with MoO_3 and without MoO_3 conditions. A peak in m/e 45, for example, is observed in the flash desorption. Its intensity, however, is the same whether MoO_3 is present or not. 3. When the experiment is run with MoO_3 in the bottom chamber, but without sieves in the top chamber, no peaks are observed at any mass. 4. The area under the H_2O desorption curve, corrected for background H_2O, varies in proportion to the mass of the MoO_3 pellet. The control experiments convincingly demonstrate that water is produced by the interaction of ethyl alcohol with MoO_3 at room temperature and can be trapped and concentrated by this simple GC/MS-type arrangement.

The water desorption data were calibrated by using identical sieve samples in the top chamber of the apparatus and in the microbalance pan. Both sets of sieves were simultaneously exposed to water vapor from the manifold. Uptake of H_2O by the sieves on the balance pan was measured gravimetrically. Water desorbed during flash heating of the sieves in the chamber was measured in the usual way. The resulting calibration curve (m/e 18 integral vs. chemisorption mass of H_2O) is shown in Figure 3.

The MoO_3 powder used in this study was synthesized by decomposing molybdenum oxalate in air at 400 °C. The N_2 BET surface area of the

Table I. Chemisorption and Catalyst Reduction by Various Alcohols on MoO_3[a]

adsorbate	uptake μg	uptake, no./ $cm^2 \times 10^{-13}$	O atom loss, μg	reduction efficiency
CH_3OH	48 (±4)	10.5	11 (±2)	0.47 (±0.10)
CH_3CH_2OH	71 (±5)	10.8	15 (±2)	0.60 (±0.10)
$(CH_3)_2CHOH$	70 (±4)	8.2	6 (±1)	0.31 (±0.10)
$(CH_3)_3COH$	32 (±3)	3.0	0 (±2)	0.00 (±0.10)

[a] 83.9 mg of MoO_3; BET surface area = 10.2 m^2/g; exposure of 5 torr for 30 min with each alcohol.

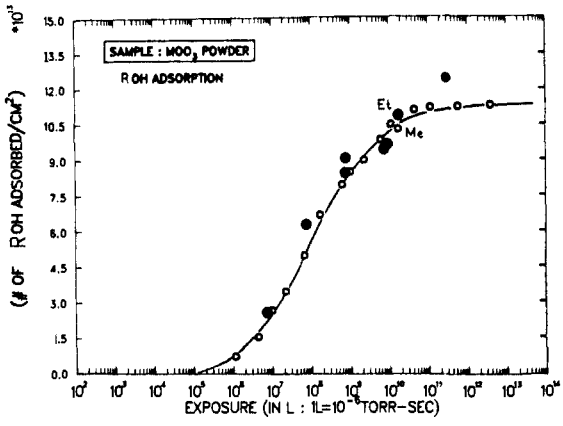

Figure 4. Methyl alcohol and ethyl alcohol molar chemisorption per unit surface area as a function of exposure: (●) ethyl alcohol, (○) methyl alcohol.

powder was approximately 10 m^2/g.[1]

Results

Table I shows chemisorption data for the alcohol series methyl, ethyl, 2-propyl, *tert*-butyl alcohols on MoO_3. Chemisorption was measured at a constant exposure of 150 torr-min and represents the stable weight gain after pump out to less than 10^{-7} torr at room temperature. Although the situation is more complicated, because chemisorption occurs by a combination of molecular and dissociative mechanisms, for a qualitative comparison, it is useful to assume molecular adsorption and compare the uptake on a molar basis. The comparative data are shown in column 3 of Table I. Chemisorption is inefficient for all these alcohols on MoO_3. Uptake as a function of exposure for methyl and ethyl alcohols is plotted in Figure 4. On a molar basis, the curves are nearly congruent. Uptake at 10^7 L ($\sim 10^{-1}$ torr-min) and 10^{11} L ($\sim 10^3$ torr-min) represents chemisorption probabilities per gas/solid collision of $\sim 10^{-8}$ and $\sim 10^{-11}$, respectively. The general form of the curves is consistent with the Elovich equation, as has previously been observed with other metal oxide systems.[3]

Infrared spectroscopy has demonstrated that metal–methoxy groups can be formed during exposure of MoO_3 to methyl alcohol at 25 °C.[4] We have quantified this process for ethyl alcohol uptake by measuring the amount of H_2O produced during chemisorption. As described in the Experimental Section, 3-Å molecular sieves are used to trap water. The amount of water formed is determined by integration of the m/e 18 peak in mass spectral analysis of the gas stream during subsequent flash desorption from the sieves. Typical data are shown in Figure 2. The curve represented by + is the m/e 18 profile after an exposure of 1.2×10^3 torr-min. The curve represented by ○ is a control experiment carried out identically but with MoO_3 absent from the dosing chamber. The difference between the two curves represents the water produced and trapped during the chemisorption of ethyl alcohol on MoO_3 at 25 °C. The mass spectral integrals are calibrated by using direct H_2O dosing experiments

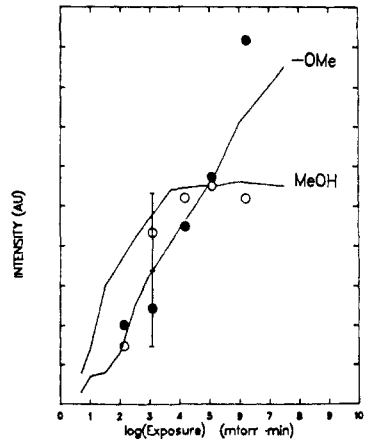

Figure 5. Deconvoluted microbalance data for the partitioning between dissociative and intact chemisorption: (●) OET(ads), (○) HOEt(ads). IR data for relative intensities of bands associated with dissociative and intact chemisorption (solid lines, data for MeOH).

Table II.

adsorbed gas	desorbed molecule (T_{max}, °C)[a]
CH_3OH	CH_3OH (100), CH_2O (215), H_2O (240)
CH_3CH_2OH	CH_3CH_2OH (100), CH_3CHO (175), H_2O (200)
$(CH_3)_2CHOH$	$(CH_3)_2CHOH$ (100, 120), $(CH_3)_2CO$ (140) CH_2CHCH_3 (150), H_2O (150)
$(CH_3)_3COH$	$CH_2C(CH_3)_2$ (75), H_2O (>80)

[a] Identified by comparison of cracking pattern with pure standards.

Scheme I

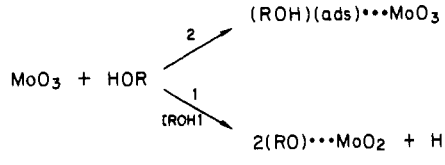

(vide infra). The calibration curve and the water production data for an ethyl alcohol exposure of 120 torr-min are shown in Figure 3. The experimental value represents the mean of three experiments at this exposure.

The combination of adsorption mass changes and H_2O production can be used together to quantitatively define the nature of the chemisorbed species. We assume that chemisorption can be represented by the stoichiometry of Scheme I. Then, assuming that all the H_2O produced is trapped, the calibration allows one to determine the total number of OEt(ads) that are formed – (2OEt(ads)/H_2O evolved). Once the number of OEt(ads) is known, the total uptake can be used to calculate the number of HOEt(ads). Deconvoluted data at several exposures are shown in Figure 5. The picture that emerges is that adsorption of intact alcohol saturates at lower exposures than dissociative chemisorption. In the high-exposure regime where total uptake begins to level off, ($\sim 10^2$ torr-min), HOEt(ads) and OEt(ads) are present in roughly comparable amounts. At very high exposures, OEt(ads) may grow at the expense of HOEt(ads). This picture is in very good agreement with IR data on the growth of methyl alcohol(ads) and OMe(ads) spectroscopic features with exposure. The IR data are shown as solid lines in Figure 5.[5] The IR curves have been normalized to fit the H_2O production data at 10^5 mtorr-min. Because of the similarity of the MeOH and EtOH chemisorption isotherms,and correspondence between the IR data on MeOH and the H_2O production data on EtOH, we conclude that Scheme I is an adequate representation of the chemisorption process with both of these alcohols.

(3) (a) Morris, M. A.; Bowker, M.; King, D. A. In *Comprehensive Chemical Kinetics*; Bamford, C. H., Tipper, C. F. H., Compton, R. G., Eds.; Elsevier: New York, Vol. 19, p 95. (b) C.; Anaroni, F. C. Tomkins, *Adv. Catal.* **1970**, *1*, 1.

(4) Groff, R. P. *J. Catal.* **1984**, *86*, 215.

(5) Staley, R. H., unpublished results. As shown in ref 4, infrared spectroscopy can be used to follow the growth of CH_3OH(ads) and CH_3O(ads) with exposure. Features that can be assigned as OH(ads) grow concurrently with CH_3OH(ads) and not with OCH_3(ads), implying that a free hydroxyl species is not present in significant concentration at the surface under these conditions.

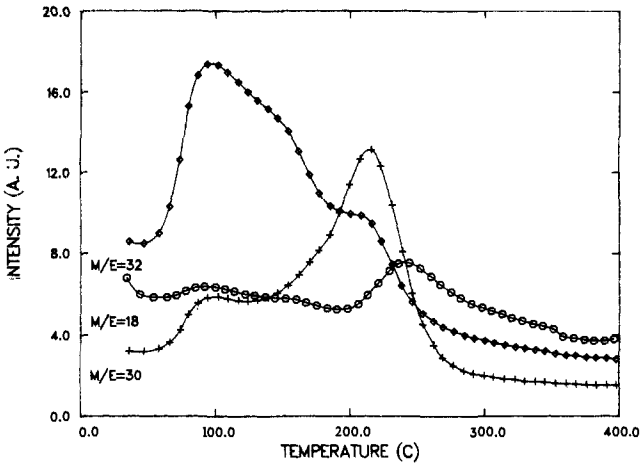

Figure 6. Temperature-programmed desorption spectrum for methyl alcohol on MoO_3. Intensities are raw ion currents for the m/e values indicated. An interpretation of these data is shown in Table II (exposure = 150 torr-min at 25 °C, heating rate = 5 °C/min).

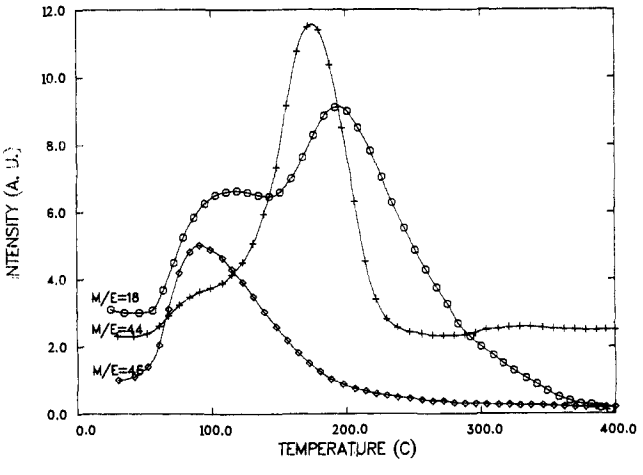

Figure 7. Temperature-programmed desorption spectrum for ethyl alcohol on MoO_3 (conditions as in Figure 6).

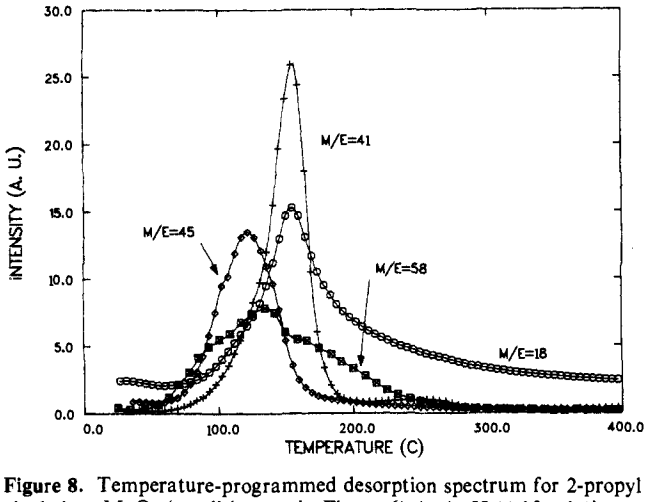

Figure 8. Temperature-programmed desorption spectrum for 2-propyl alcohol on MoO_3 (conditions as in Figure 6) (m/e 58 × 10 relative to other traces).

Following adsorption and pump down to 10^{-7} torr, the chemisorbed material was desorbed by using a linear temperature program of 5 °C/min. Intensity profiles of ions of various masses evolved during heating are shown in Figures 6–9. Each figure shows mass spectral data for a single alcohol chemisorbed at an exposure of 150 torr-min at 25 °C. Each mass is characteristic of a given neutral molecule in the gas stream, but the profiles have

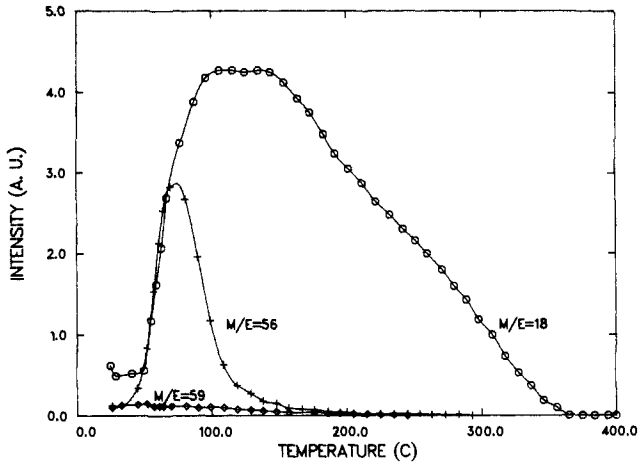

Figure 9. Temperature-programmed desorption spectrum for 2-methyl-2-propyl alcohol on MoO_3 (conditions as in Figure 6).

Scheme II

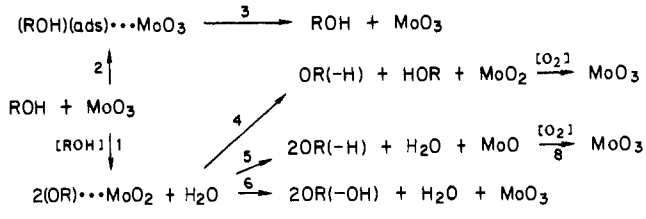

not been corrected for sensitivity differences or for contributions from fragmentation of other neutrals. Therefore, the data do not represent absolute partial pressures of desorbing vapors. However, for each figure, the following features should be noted: (1) the structures of the desorbing gases and (2) the temperature of the peak maximum for each gas. These features are listed in Table II.

Methyl, ethyl, and 2-propyl alcohols all show an α peak at ~100 °C where alcohol desorbs intact and a β peak at higher temperature where reaction products desorb. Dehydrogenation occurs exclusively with CH_3OH and is the principal reaction pathway with EtOH. Dehydration occurs to a very minor extent for EtOH but is the major pathway for 2-PrOH. t-BuOH shows only dehydration and in fact no intact t-BuOH desorbs.

There are some very informative trends in the T_{max} values. The α peak temperature is insensitive to alcohol structure. The dehydrogenation product desorbs at progressively lower temperatures in the sequence, MeOH > EtOH > 2-PrOH. When oxidation occurs as the major reaction channel (MeOH, EtOH), H_2O desorbs at a somewhat higher temperature than the carbonyl compound. When dehydration occurs as the major reaction channel (2-PrOH, t-BuOH), H_2O desorbs at nearly the same temperature as the organic product. The T_{max} of the dehydration product decreases in the sequence EtOH > 2-PrOH > t-BuOH.

After temperature-programmed reaction, there has been a net weight loss in the catalyst for all alcohols except t-BuOH. This mass can be completely restored by reoxidation and therefore represents the oxygen loss from MoO_3 accompanying product desorption. The number of oxygen atoms required to restore the catalyst mass and the ratio of this number to the number of alcohol molecules bound at room temperature is shown in Table I. The extent of catalyst reduction increases in the order EtOH > MeOH > 2-PrOH > t-BuOH. The efficiency of catalyst reduction per alcohol adsorbed shows the same trend. The inefficient redution by 2-PrOH and the lack of reduction by t-BuOH are clearly consistent with the observed products, since dehydration can occur by a nonredox pathway.

Discussion

In order to describe the entire catalytic cycle of adsorption, temperature-programmed reaction, and reoxidation, we may extend Scheme I As Scheme II.

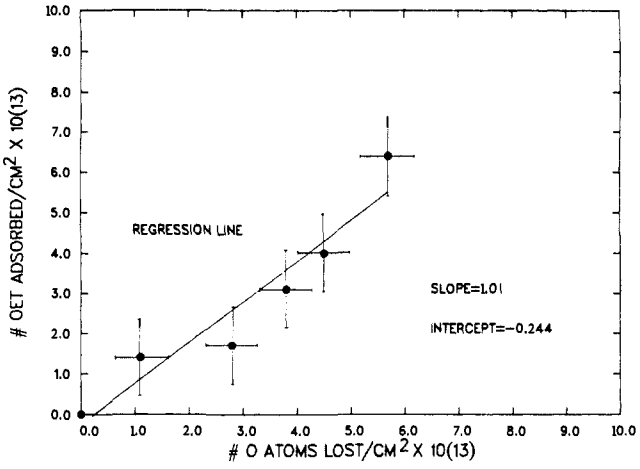

Figure 10. Correlation between number of ethoxy groups bound during chemisorption stage at 25 °C and number of oxygen atoms lost from the catalyst during heating to 400 °C.

In this scheme, oxidation products appear as OR(–H) and dehydration products as OR(–OH). This representation is chosen in order to emphasize the stoichiometric relationships among the elementary steps in this scheme. The essential features of this scheme are as follows: (1) Adsorption occurs as a combination of intact and dissociative processes. (2) Only alcohol first adsorbed as alkoxy is oxidized, OR(–H). (3) The competition among reactions 4, 5, and 6 determines the product distribution in the β peak and the extent of catalyst reduction.

For ethyl alcohol, our data provide excellent evidence for the carbon, hydrogen, and oxygen stoichiometry of this scheme. Figure 10 shows the correlation between the number of ethoxy molecules formed and the number of oxygen atoms required for reoxidation. Within experimental error, a 1:1 stoichiometry is implied. This is consistent with Scheme II when reaction 5 dominates the competition during TPD. Reaction 4 would predict a ratio of 1/2 "O" atoms lost per OR formed. Reaction 6 predicts no catalyst reduction. Mass spectroscopy during the TPD of ethyl alcohol also shows the dominance of reaction 5. Insignificant amounts of intact alcohol (ROH in Scheme II) or ethylene (OR(–OH) in Scheme II) are observed in the β peak TPD region. In previous work, we showed that there is a linear relationship between O atom loss and the integrated intensity of the formaldehyde peak in TPD of methyl alcohol over MoO_3.[1] The same is true for acetaldehyde in ethyl alcohol TPD. Since OEt formation and O atom loss have already been linked in Figure 10, a 1:1 correlation between OEt formation and acetaldehyde production is also implied.

For the other alcohols, the data are less complete and the stoichiometry cannot be mapped out so quantitatively. However, the changes observed in both product distribution and the extent of reduction can be satisfactorily explained within the framework of Scheme II. For methyl alcohol, for example, Figure 6 shows a more pronounced alcohol peak in the β region than with ethyl alcohol. In terms of Scheme II, this observation implies that reaction 4 competes more effectively with reaction 5 in methoxy desorption than in ethoxy desorption. A reasonable explanation would be as follows. The rate of decomposition of the surface methoxy or ethoxy is limited by C–H bond breaking. A transient population of surface hydroxyls is formed as a result of C–H cleavage. Reaction 5 corresponds to a condensation of these surface hydroxyls to form water. Reaction 4 corresponds to a hydroxyl–alkoxyl recombination to desorb alcohol. When the transient hydroxyl concentration builds up at a lower temperature, as in ethoxy decomposition, both condensation rate constants, k_5 to water or k_4 to alcohol, are small. This tends to increase the steady-state concentration of hydroxyls and favor the process that is second order in hydroxyl, reaction 5, relative to the process that is first order in hydroxyl, reaction 4.

This rationale is also adequate to explain the O atom weight loss data shown in Table I. For the same exposure, leading to very similar molar alcohol uptake, there are fewer O atoms lost in methyl alcohol TPD than in ethyl alcohol TPD. Since reaction 4 is not as strongly reducing as reaction 5, this observation is consistent with the diversion of some OMe(ads) along this channel during heating.

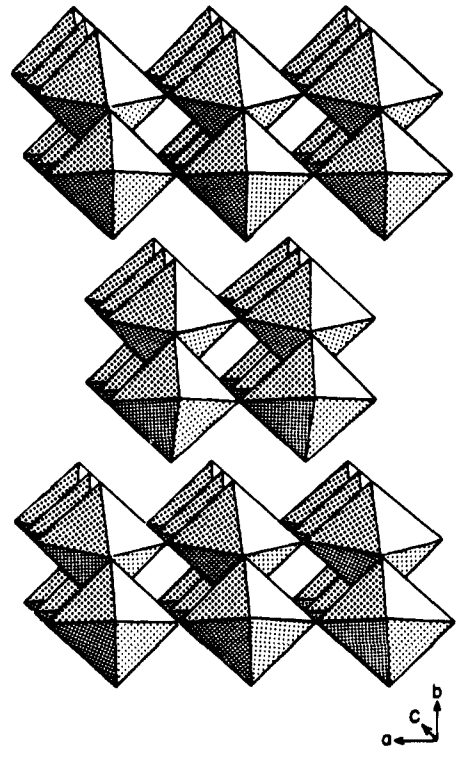

Figure 11. Representation of the structure of MoO_3 as bilayers of corner or edge-sharing octahedra. Each corner is occupied by an O atom. Each octahedral center is occupied by Mo.

For 2-propyl and *tert*-butyl alcohols, data that could be used to indicate the relative proportions of intact and dissociative chemisorptions are not available. Because the α and β peak regions are not well-resolved, it is possible that dehydration occurs from an intact adsorbed precursor. This possibility is not represented in Scheme II. Certainly, plausible routes to dehydration products could be written starting from either intact adsorbed alcohol or from surface alkoxy groups.[6] In either case, however, no catalyst reduction should accompany the formation of these products. Accordingly, there is no weight loss during TPD with *tert*-butyl alcohol and a considerably smaller weight loss for 2-propyl alcohol than for either of the primary alcohols (Table I).

Defining the stoichiometry of the cycle with respect to molybdenum is somewhat more difficult. However, as we have previously argued, it seems likely that the majority of Mo atoms in the outermost layer are not active in catalysis.[1] At a stoichiometry of 1 chemisorbed molecule per Mo atom, the number of Mo atoms involved in the chemisorption at an exposure of 10 Torr/30 min (near saturation) would be 1.1×10^{14}/cm^2 for methyl alcohol 1.2×10^{14}/cm^2 for ethyl alcohol, 8.2×10^{13}/cm^2 for 2-propyl alcohol, and 3.0×10^{13}/cm^2 for *tert*-butyl alcohol. The number of Mo atoms involved in alkoxide binding, the only catalytically important chemisorption, would be $\sim 7 \times 10^{13}$/cm^2 for methyl and ethyl alcohols, $\sim 3.5 \times 10^{13}$/cm^2 for 2-propyl alcohol, and $< 3 \times 10^{13}$/cm^2 for *tert*-butyl alcohols, assuming that the 1:1 correlation of O atom loss to ethoxy binding applies to 2-propyl alcohol as well. If the stoichiometry for chemisorption of methoxy were 2 methoxy per Mo atom, then only about 3.5×10^{13}/cm^2 Mo atoms would be implicated.

(6) One possible clue to the structure of the adsorbed precursor is the small difference in T_{max} between the olefin and water peaks in TPD. When oxidation occurs, the associated water appears at a substantially higher temperature. This may suggest a concerted loss of water from intact adsorbed alcohol during dehydration.

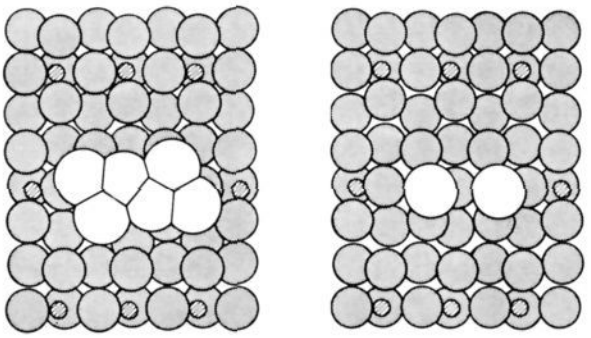

Figure 12. Representation of metal–alkoxide intermediates on adjacent metal atom sites on the [100] face of MoO_3. Standard ionic radii for Mo^{6+} (0.59 Å) and O^{2-} (1.35 Å). Standard van der Waals radii for CH_3 (1.70 Å) (O).

In order to give these data some chemical meaning, we require a structural model for the surface of the solid. The bulk structure of MoO_3 is a very interesting one.[7] It can be thought of as a stack of bilayers of edge-sharing MoO_6 octahedra (Figure 11). Termination parallel to the layers, between adjacent bilayers, exposes the coordinately saturated [010] surface. Termination perpendicular to the layers in either the [100] or the [001] direction leaves oxygen vacancies at the surface. As this picture would suggest, it is well-known that the stable cleavage plane of MoO_3 is the [010] surface.[8] SEM shows our sample to consist of platelet-shaped particles with latitudinal dimension of a few micrometers and longitudinal dimension that is perhaps 20% of that. This implies that the ratio of the [010], latitudinal surface to the non-[010] longitudinal surfaces is >2.0. From the bulk crystal data, one may determine that the number of Mo atoms in the outermost metal layer on a perfect [010] surface is $6.8 \times 10^{14}/cm^2$. On other surfaces, because cleavage leaves alternating Mo and O atoms in the exposed atomic layer, the number of Mo in the outermost plane is less $\sim 3.6 \times 10^{14}/cm^2$. The Mo atoms available at the surface, therefore, can be described as $\geq 4.6 \times 10^{14}/cm^2$ [010] and $\leq 1.2 \times 10^{14}/cm^2$ non-[010]. The saturation coverages of methoxide or ethoxide are consistent with an inactive [010] surface and localized dissociative chemisorption on non-[010] faces. We have suggested this type of surface structure sensitivity in methyl alcohol oxidation over MoO_3 in previous work.[1,9] Of course, because of the possibility of reconstruction and surface defects, the true surface structure at the binding site is difficult, at best, to determine directly. However, as has been pointed out by others, the consideration of ideal cleavage planes can provide a framework for systematizing structure/reactivity data for heterogeneous chemistry on oxides.[10]

The fall off in chemisorption capacity of the surface with increasing size of the alkyl group is consistent with a steric effect. The larger alcohols may saturate at lower coverages due to repulsive interactions between alkoxy groups bound at neighboring metal atoms. Space-filling diagrams for OMe and O-*t*-Bu binding to adjacent metal atom sites on [001] are shown in Figure 12. The clear difference in spatial requirements of the two ligands is apparent. While the methoxy groups (on the right) are beyond van der Waals contact, the *tert*-butoxy groups (on the left) appear badly constrained. The extreme sensitivity of metal–alkoxide chemistry to the steric bulk of the alkoxy ligands is well-known in metal cluster chemistry.[11]

The oxidative decomposition of the surface alkoxyl, reaction 5, requires cleavage of an α-C–H bond. Isotope-labeling studies have shown that T_{max} increases by ~25 °C when H is replaced by D at this position.[12] The progressive decrease in T_{max} of the oxidation product as CH_3 replaces H at the α carbon parallels changes in that C–H bond dissociation energy. In the gas phase, the decomposition of alkoxy radicals by H atom loss becomes less endothermic in the sequence MeO· > EtO· > *i*-PrO. The increment is about 4 kcal/mol per methyl for H substitution.[13] This is of the correct order of magnitude to give the observed changes in T_{max}.

Alkoxides are generaly regarded as π-donor ligands.[14] Thus, an appropriate partial structure for the binding represented in Figure 12 should include some contribution from dipolar forms:

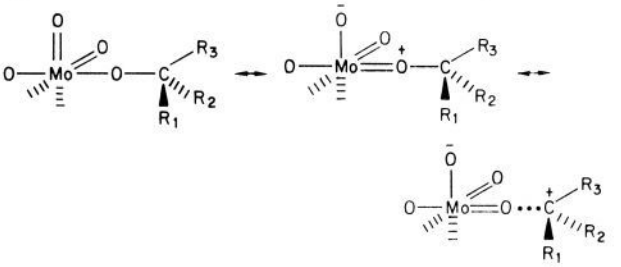

As hydrogens are progressively replaced by methyls in R_1, R_2, and R_3, the importance of these dipolar forms should increase since the larger hydrocarbons are more stable as electron-deficient carbonium-ion-like species. One may rationalize the emergence of reaction 6 for decomposition of an 2-propoxide intermediate due to this enhanced carbonium ion character.

Conclusions

The chemisorption and temperature-programmed reaction spectroscopies of ethyl, 2-propyl, and *tert*-butyl alcohols over MoO_3 are consistent with expectations based on a mechanistic model previously developed to understand methyl alcohol chemistry. The significant differences in steric and electronic properties of the alcohols in this series are manifested in differences in the amount of chemisorption, the product distribution, and the peak desorption temperatures. In no case does the saturation chemisorption exceed what would be expected on the basis of localized adsorption on non-[010] faces at room temperature. There is a clear drop off in the chemisorption capacity of the MoO_3 powder as the size of the hydrocarbon moiety of the alcohols increases. This trend can be satisfactorily rationalized as a steric effect.

The catalytically important intermediate in the partial oxidation chemistry is a surface metal–alkoxide. The central role of metal–alkoxide intermediates in molybdate-based oxidation chemistry echoes the conclusions of Madix et al. for alcohol oxidation over copper[15] and, in fact, is precedented by group VIA (6) oxidations in both homogeneous[16] and enzymatic media.[17] For ethyl alcohol, we have directly demonstrated that the formation of alkoxy groups on the MoO_3 surface can occur at 25 °C with concurrent loss of water. The number of alkoxide groups formed has been measured and linked quantitatively to (1) oxygen atom loss from the catalyst during TPRS, (2) yields of oxidation product, and (3) infrared spectral measurements of –OR(ads) and HOR-(ads) concentrations. Future work will be directed toward more specific structural characterization of the active site region and more quantitative linkage of the surface science to reactor kinetics.

Acknowledgment. We thank Willis Dolinger for his able technical assistance and Dr. U. Chowdhry for preparation of the MoO_3.

(7) Hulliger, F. *Structural Chemistry of Layer-Type Phases*; Levy F., Ed.; D. Reidel: Boston, 1976; Vol. 5, p 169.
(8) Firment, L. E.; Ferretti, A. *Surf. Sci.* **1983**, *129*, 155.
(9) Chowdhry, U.; Ferretti, A. Firment, L. E.; Machiels, C. J.; Ohuchi, F.; Sleight, A. W.; Staley, R. H. *Appl. Surf. Sci.* **1984**, *19*, 360.
(10) (a) Stone, F. S. *J. Solid State Chem.* **1975**, *12*, 271. (b) Henrich, V. E. *Prog. Surf. Sci.* **1983**, *14*, 175.
(11) (a) Chisholm, M. H.; Folting, K.; Huffman, J. C.; Tatz, R. J. *J. Am. Chem. Soc.* **1984**, *106*, 1153. (b) Chisholm, M. C.; Hoffman, D. M.; Huffman, J. C. *J. Am. Chem. Soc.* **184**, *106*, 6806 and references therin.
(12) Machiels, C. J.; Sleight, A. W. *J. Catal.* **1982**, *76*, 238.
(13) Benson, S. W. *Thermochemical Kinetics*; Wiley: New York, 1976.
(14) (a) Coffindaffer, T. W.; Rothwell, I. P.; Huffman, J. C. *Inorg. Chem.* **1983**, *22*, 2906. (b) Lubben, T. V.; Wolczanski, P. T.; Van Duyne, G. D. *Organometallics* **1984**, *3*, 977.
(15) Bowker, M.; Madix, R. J. *Sur. Sci.* **1982**, *116*, 549.
(16) March, J. *Advanced Organic Chemistry*; McGraw-Hill: New York, 1977; p 1083.
(17) Sheldon, R. A.; Kochi, J. K. *Metal-Catalyzed Oxidations of Organic Compounds*; Academic: New York, 1981; p 242.